AN EFFICIENT ONE-STEP TAYLOR-GALERKIN SCHEME TO ANALYZE 3-D HIGH COMPRESSIBLE FLOWS USING THE FINITE ELEMENT METHOD

Horacio P. Burbridge – willybur@ssdnet.com.ar
Armando M. Awruch – amawruch@adufrgs.ufrgs.br
Programa de Pós-graduação em Engenharia Civil, Universidade Federal do Rio Grande do Sul, Av. Osvaldo Aranha 99, 3° Andar, Porto Alegre, RS, Brasil.

Abstract. *An algorithm to simulate 3-D high compressible flows of viscous and non-viscous fluids is presented in this work. The time integration procedure was obtained from an expansion in Taylor series of the governing equations, while spatial discretization was carried out using the Finite Element Method (FEM) based on the classical Bubnov-Galerkin technique. In order to obtain considerable improvements in CPU time and memory, and to take advantage from the fast vectorial processors existing in modern supercomputers, an analytical evaluation of element matrices was adopted, deriving the corresponding expressions from the eight-node isoparametric brick element. One practical example is also presented in this paper in order to show the excellent computational performance and the good agreements with results obtained previously by other authors.*

Keywords: *Computational fluid dynamics, Compressible flows, Finite element method, Taylor-Galerkin.*

1. INTRODUCTION

Computational Fluid Dynamics (CFD) has become a subject of increasing importance in the last three decades due to factors such as the rapid rate of developments in computer technology, improvements in the quality of numerical algorithms and the potential of this field to deal with “real world” phenomena that cannot be reproduced so easily by physical model tests.

Even though Finite Differences and Finite Volumes have been traditionally employed in CFD and that the Boundary Element Method has also been played an important role in the last twenty years, the Finite Element Method (FEM) has become an efficient alternative technique to analyze Fluid Dynamics problems since Zienkiewicz and Cheung (1965) published their first work in this area.

The main objectives of this work are the development of an efficient finite element formulation and application of a numerical algorithm to simulate three-dimensional high compressible flows.

An one step Taylor-Galerkin scheme and the Finite Element Method were used for time and spatial discretization. In order to get important savings in CPU time and computer memory and to obtain considerable improvements in the code vectorization, an analytical

evaluation of the element matrices was performed. The corresponding expressions were derived from the eight-node hexahedral isoparametric element. The Taylor-Galerkin scheme, which may be interpreted as the finite element version of the Lax-Wendroff scheme used in finite differences (Richtmayer and Morton, 1967), was previously used by Donea (1984), Löhner et al. (1985), Morgan et. al. (1991) and Texeira et. al. (1998), among others.

In order to stabilize numerically the solution in the presence of strong shocks, it is necessary to add numerical damping to the flow solver. Two main possibilities may be employed: the flux corrected transport method (FCT) as presented by Löhner (1988) and the artificial viscosity model, as given by Argyris et. al. (1989). In this work the last alternative was adopted because of its simplicity and efficiency in terms of CPU time.

2. THE GOVERNING EQUATIONS

In an Eulerian description the system of partial differential equations governing fluid dynamics problems can be written as follows:

$$\frac{\partial \mathbf{U}}{\partial t} + \frac{\partial \mathbf{F}_i}{\partial x_i} + \frac{\partial \mathbf{G}_i}{\partial x_i} = \mathbf{0} \qquad \text{in } \Omega \tag{1}$$

with

$$\mathbf{U} = \begin{Bmatrix} \rho \\ \rho v_1 \\ \rho v_2 \\ \rho v_3 \\ \rho e \end{Bmatrix}, \quad \mathbf{F}_i = \begin{Bmatrix} \rho v_i \\ \rho v_1 v_i + p\delta_{i1} \\ \rho v_2 v_i + p\delta_{i2} \\ \rho v_3 v_i + p\delta_{i3} \\ v_i(\rho e + p) \end{Bmatrix}, \quad \mathbf{G}_i = \begin{Bmatrix} 0 \\ -\tau_{i1} \\ -\tau_{i2} \\ -\tau_{i3} \\ -\tau_{ij} v_j - K \dfrac{\partial u}{\partial x_i} \end{Bmatrix} \tag{2}$$

where v_i are the fluid velocity components, ρ is the density (specific mass), p is the thermodynamic pressure, τ_{ij} are the viscous components of the stress tensor, e and u are the specific total energy and the specific internal energy respectively, K is the thermal conductivity, δ_{ij} is the Kronecker delta, Ω is the domain to be studied and, finally, x_i and t are the spatial and temporal coordinates respectively. In those expressions isotropic heat diffusion was assumed. For a Newtonian fluid the viscous stress components are given by:

$$\tau_{ij} = \mu\left[\frac{\partial v_i}{\partial x_j} + \frac{\partial v_j}{\partial x_i}\right] + \lambda \frac{\partial v_k}{\partial x_k}\delta_{ij} \qquad (i,j,k = 1,2,3) \tag{3}$$

where μ and λ are the shear and the volumetric viscosity respectively.

The equation of state can be written as:

$$p = (\gamma - 1)\rho u \tag{4}$$

with $\gamma = c_v / c_p$, where c_v and c_p are the specific heat coefficients at constant volume and pressure, respectively. The internal energy and the temperature are related to the independent field variables by the following expression

$$u = c_v T = e - \tfrac{1}{2} v_i v_i \tag{5}$$

where u and T are the specific internal energy and the temperature, respectively.

Dimensionless variables are used in this work, with

$$\underline{t} = t\frac{c_{ref}}{L_{ref}}, \quad \underline{x_i} = \frac{x_i}{L_{ref}}, \quad \underline{v_i} = \frac{v_i}{c_{ref}}, \quad \underline{\rho} = \frac{\rho}{\rho_{ref}}, \quad \underline{p} = \frac{p}{\rho_{ref} c_{ref}^2}, \quad \underline{e} = \frac{e}{c_{ref}^2}, \quad \underline{u} = \frac{c_v T}{c_{ref}^2} \tag{6}$$

where L_{ref} is a reference length, c_{ref} is the reference value of the sound speed and ρ_{ref} is the reference value of specific mass (c_{ref} and ρ_{ref} are values of c and ρ at the far field, where the flow has not any perturbation).

Sutherland's law is used in this work to establish the dependence of the shear viscosity, volumetric viscosity and the conductivity coefficient with respect to the temperature. In dimensionless form, this law may be expressed as

$$\underline{\mu} = \frac{\mathrm{M}_{ref}}{\mathrm{Re}_{ref}} \frac{\underline{S} + \underline{u_{ref}}}{\underline{S} + \underline{u}} \left(\frac{\underline{u}}{\underline{u_{ref}}} \right)^{\frac{3}{2}} \tag{7}$$

$$\underline{\lambda} = -2/3\,\underline{\mu} \tag{8}$$

$$\underline{K} = \frac{\mathrm{M}_{ref}\,\gamma}{\mathrm{Re}_{ref}\,\mathrm{Pr}_{ref}} \frac{\underline{S_K} + \underline{u_{ref}}}{\underline{S_K} + \underline{u}} \left(\frac{\underline{u}}{\underline{u_{ref}}} \right)^{\frac{3}{2}} \tag{9}$$

with

$$\underline{S} = \frac{c_v S}{{c_{ref}}^2}, \quad \underline{S_K} = \frac{c_v S_K}{{c_{ref}}^2} \tag{10}$$

where M_{ref}, Re_{ref} and Pr_{ref} are reference values of Mach, Reynolds and Prandtl numbers, respectively. Values for S_K and S can be found in White (1974). All variables considered in the remaining of this work will be dimensionless but, to simplify notation, the bars used under these variables, as indicated in Eqs. (6) to (10), will be eliminated.

In order to get a well-posed problem, boundary and initial conditions must be added to Eq. (1). Forced boundary conditions (or Dirichlet boundary conditions) are given by

$$v_i = \overline{v_i} \qquad \text{on} \quad \Gamma_v \tag{11}$$

$$\rho = \overline{\rho} \qquad \text{on} \quad \Gamma_\rho \tag{12}$$

$$u = \overline{u} \qquad \text{on} \quad \Gamma_u \tag{13}$$

where $\overline{v_i}$, $\overline{\rho}$ and $\overline{u}$ are prescribed values of velocity components, specific mass and specific internal energy, at the parts of the boundary surface denoted by Γ_v, Γ_ρ and Γ_u, respectively.

Natural boundary conditions (or Newmann boundary conditions) are given by

$$\left(-p\delta_{ij} + \tau_{ij}\right) n_j = \hat{t}_i \qquad \text{on} \quad \Gamma_\sigma \tag{14}$$

and

$$K\frac{\partial T}{\partial x_i} n_i = \hat{q} \qquad \text{on} \quad \Gamma_q \tag{15}$$

where n_i are de cosines of the angles formed by the normal vector to the surface Γ_σ or Γ_q and the global reference axes x_i. In Eqs (14) and (15) $\hat{t}_i$ are the components of the surface load acting on Γ_σ and $\hat{q}$ is the normal heat flux acting as distributed sources on Γ_q. Effects of radiation and convection at the surface boundaries have not been considered.

For non-viscous fluids the term $\partial \mathbf{G}_i / \partial x_i$ in Eq. (1) is omitted. In this case, only the component of the velocity in the normal direction is prescribed on the solid boundary surfaces and only normal components of boundary surface loads are considered.

3. FINITE ELEMENT FORMULATION OF THE TAYLOR-GALERKIN SCHEME

Expanding the vector **U** in Taylor series and evaluating the first and second derivatives of **U** at $n+1/2$ the following expression is obtained

$$\begin{aligned}\Delta \mathbf{U}_{\mathrm{I}+1}^{n+1} = \Delta t \left[-\frac{\partial \mathbf{F}_i}{\partial x_i}^n - \frac{\partial \mathbf{G}_i}{\partial x_i}^n + \frac{\Delta t}{2} \frac{\partial}{\partial x_k} \left(v_k^n \frac{\partial \mathbf{F}_i}{\partial x_i}^n \right) \right] + \\ + \frac{\Delta t}{2} \left[-\frac{\partial \Delta \mathbf{F}_{i\,\mathrm{I}}}{\partial x_i}^{n+1} - \frac{\partial \Delta \mathbf{G}_{i\,\mathrm{I}}}{\partial x_i}^{n+1} + \frac{\Delta t}{2} \frac{\partial}{\partial x_k} \left(v_k^n \frac{\partial \Delta \mathbf{F}_{i\,\mathrm{I}}}{\partial x_i}^{n+1} \right) \right]\end{aligned} \tag{16}$$

where I is an iteration counter and *i,j,k*=1,2,3. Then, applying the classical Bubnov-Galerkin technique to Eq. (16) in the context of the Finite Element Method, the following matrix equations are obtained:

Continuity equation:

$$\{\Delta \rho\}_{\mathrm{I}+1}^{n+1} = \Delta t [\mathrm{M_D}]^{-1} \left(- [\mathrm{B^C}] \{\mathrm{F}_i^{\rho}\}^n + \frac{\Delta t}{2} \{\mathrm{g}^{\rho}\}^n \right) + \frac{\Delta t}{2} [\mathrm{M_D}]^{-1} \left(- [\mathrm{B^C}] \{\Delta \mathrm{F}_i^{\rho}\}_{\mathrm{I}}^{n+1} \right) \tag{17}$$

Momentum conservation:

$$\begin{aligned}\{\Delta \rho v_j\}_{\mathrm{I}+1}^{n+1} = \Delta t [\mathrm{M_D}]^{-1} \left(- [\mathrm{B^C}] \{\mathrm{F}_{ij}^{\rho v}\}^n - [\mathrm{D}]_{ij} \{v_i\}^n + \{\mathrm{f}_j\}^n + \frac{\Delta t}{2} \{\mathrm{g}_j^{\rho v}\}^n \right) + \\ + \frac{\Delta t}{2} [\mathrm{M_D}]^{-1} \left(- [\mathrm{B^C}] \{\Delta \mathrm{F}_{ij}^{\rho v}\}_{\mathrm{I}}^{n+1} - [\mathrm{D}]_{ij} \{\Delta v_i\}_{\mathrm{I}}^{n+1} \right)\end{aligned} \tag{18}$$

Energy equation:

$$\begin{aligned}\{\Delta \rho e\}_{\mathrm{I}+1}^{n+1} = \Delta t [\mathrm{M_D}]^{-1} \left(- [\mathrm{B^C}] \{\mathrm{F}_i^{\rho e}\}^n - [\mathrm{E}]_i \{v_i\}^n - [\mathrm{K}] \{u\}^n + \{\mathrm{q}\}^n + \frac{\Delta t}{2} \{\mathrm{g}^{\rho e}\}^n \right) + \\ + \frac{\Delta t}{2} [\mathrm{M_D}]^{-1} \left(- [\mathrm{B^C}] \{\Delta \mathrm{F}_i^{\rho e}\}_{\mathrm{I}}^{n+1} - [\mathrm{E}]_i \{\Delta v_i\}_{\mathrm{I}}^{n+1} - [\mathrm{K}] \{\Delta u\}_{\mathrm{I}}^{n+1} \right)\end{aligned} \tag{19}$$

where:

$$[\mathrm{B^C}] = [\mathrm{B}]_i + \frac{\Delta t}{2} [\mathrm{C}]_i = \int_{\Omega_E} [\Phi]^{\mathrm{T}} \frac{\partial [\Phi]}{\partial x_i} \, d\Omega + \frac{\Delta t}{2} \int_{\Omega_E} \left([\Phi] \{v_k\} \right) \frac{\partial [\Phi]^{\mathrm{T}}}{\partial x_k} \frac{\partial [\Phi]}{\partial x_i} \, d\Omega \tag{20}$$

with *i,j,k*=1,2,3, and

$$[\mathrm{D}]_{ij} = \begin{cases} \displaystyle\int_{\Omega_E} \mu\left(2+\frac{\lambda}{\mu}\right)\frac{\partial[\Phi]^{\mathrm{T}}}{\partial x_i}\frac{\partial[\Phi]}{\partial x_{(i)}}\,d\Omega + \int_{\Omega_E} \mu\,\frac{\partial[\Phi]^{\mathrm{T}}}{\partial x_k}\frac{\partial[\Phi]}{\partial x_k}\,d\Omega\,, & \text{if } i=j, \text{ and: } \begin{cases} i=1 \to k=2,3 \\ i=2 \to k=1,3 \\ i=3 \to k=1,2 \end{cases} \\ \displaystyle\int_{\Omega_E} \mu\,\frac{\partial[\Phi]^{\mathrm{T}}}{\partial x_i}\frac{\partial[\Phi]}{\partial x_j}\,d\Omega + \int_{\Omega_E} \lambda\,\frac{\partial[\Phi]^{\mathrm{T}}}{\partial x_j}\frac{\partial[\Phi]}{\partial x_i}\,d\Omega\,, & \text{if } i \neq j \end{cases} \tag{21}$$

$$[\mathrm{E}]_{\cdot} = \int_{\Omega_E} \left[\mu\left([\Phi]\{v_i\}^n\right)\frac{\partial[\Phi]^{\mathrm{T}}}{\partial x_k}\frac{\partial[\Phi]}{\partial x_k} + \mu\left([\Phi]\{v_k\}^n\right)\frac{\partial[\Phi]^{\mathrm{T}}}{\partial x_i}\frac{\partial[\Phi]}{\partial x_k} + \lambda\left([\Phi]\{v_k\}^n\right)\frac{\partial[\Phi]^{\mathrm{T}}}{\partial x_k}\frac{\partial[\Phi]}{\partial x_i} \right] d\Omega \tag{22}$$

$$[\mathrm{K}] = \int_{\Omega_E} K\,\frac{\partial[\Phi]^{\mathrm{T}}}{\partial x_i}\frac{\partial[\Phi]}{\partial x_i}\,d\Omega \tag{23}$$

$$[\mathrm{M_D}] = \begin{cases} \Omega_E \big/ 8 & \text{for main diagonal terms} \\ 0 & \text{for all off - diagonal terms} \end{cases} \tag{24}$$

$$\{\mathrm{F}_i^{\rho}\} = \{\rho v_i\}, \quad \{\mathrm{F}_{ij}^{\rho v}\} = \{\rho v_i v_j + p\delta_{ij}\}, \quad \{\mathrm{F}_i^{\rho e}\} = \{\rho e v_i + p v_i\} \tag{25}$$

$$\{g^{\rho}\}^n = \int_{\Gamma_E} [\Phi^*]^{\mathrm{T}}\left([\Phi]\{v_k\}^n\right) n_k \left(\frac{\partial[\Phi]}{\partial x_i}\{\mathrm{F}_i^{\rho}\}^n\right) d\Gamma \tag{26}$$

$$\{g_j^{\rho v}\}^n = \int_{\Gamma_E} [\Phi^*]^{\mathrm{T}}\left([\Phi]\{v_k\}^n\right) n_k \left(\frac{\partial[\Phi]}{\partial x_i}\{\mathrm{F}_{ij}^{\rho v}\}^n\right) d\Gamma \tag{27}$$

$$\{g^{\rho e}\}^n = \int_{\Gamma_E} [\Phi^*]^{\mathrm{T}}\left([\Phi]\{v_k\}^n\right) n_k \left(\frac{\partial[\Phi]}{\partial x_i}\{\mathrm{F}_i^{\rho e}\}^n\right) d\Gamma \tag{28}$$

$$\{f_j\}^n = \int_{\Gamma_E} [\Phi^*]^{\mathrm{T}}\left[\mu\left(\frac{\partial[\Phi]}{\partial x_i}\{v_j\}^n + \frac{\partial[\Phi]}{\partial x_j}\{v_i\}^n\right) + \lambda\left(\frac{\partial[\Phi]}{\partial x_k}\{v_k\}^n\right)\delta_{ij}\right] n_i\, d\Gamma \tag{29}$$

$$\begin{aligned} \{q\}^n = & \int_{\Gamma_E} [\Phi^*]^{\mathrm{T}}\left([\Phi]\{v_j\}^n\right)\left[\mu\left(\frac{\partial[\Phi]}{\partial x_i}\{v_j\}^n + \frac{\partial[\Phi]}{\partial x_j}\{v_i\}^n\right) + \lambda\left(\frac{\partial[\Phi]}{\partial x_k}\{v_k\}^n\right)\delta_{ij}\right] n_i\, d\Gamma + \\ & + \int_{\Gamma_E} [\Phi^*]^{\mathrm{T}} K\left(\frac{\partial[\Phi]}{\partial x_i}\{u\}^n\right) n_i\, d\Gamma \end{aligned} \tag{30}$$

In this expressions Ω_E and Γ_E are element volume and boundary surface respectively, $[\Phi] = [\Phi_1 \quad \Phi_2 \quad \ldots \quad \Phi_8]$ is the vector containing the shape functions for each node, $[\Phi^*]$ is the vector containing the shape functions evaluated on the contour surface and $[\mathrm{M_D}]$ is the lumped mass matrix.

After assembling the Eqs. (17), (18) and (19) and applying the corresponding boundary conditions, the nodal values of ρ, ρv_j and ρe can be computed at each time level using an

iterative scheme. Nodal values of the thermodynamic pressure are calculated with the equation of state, i.e. Eq.(4). Finally, nodal values of velocity components, specific total energy, specific internal energy and temperature may also be computed. For non-viscous fluids, matrices $[\mathrm{D}]_{ij}$, $[\mathrm{E}]_i$ and $[\mathrm{K}]$ and vectors $\{f_j\}$ and $\{q\}$ are omitted.

The Courant stability condition for each element in dimensionless form is given by

$$\Delta t_E = \beta \frac{\dfrac{L_E}{L_{ref}}}{M + \dfrac{c}{c_{ref}}} \qquad E=1,2,....,\mathrm{NEM} \tag{31}$$

where NEM is the total number of elements in the finite element mesh, L_E is a characteristic dimension of the element, c is the sound speed, M is the local Mach number and β is a safety coefficient (in this work was adopted $\beta = 0.2$ or $\beta = 0.3$). Equations (17), (18) and (19) were applied with an uniform value of Δt on the whole finite element mesh, adopting the smallest value between all Δt_E obtained applying Eq. (31) to all mesh elements.

In order to capture strong discontinuities and eliminate high frequency oscillations near shock waves, an artificial viscosity is used. The smoothed solution is obtained from the non-smoothed solution applying the following expression:

$$\{\mathbf{U}_s\}^{n+1} = \{\mathbf{U}\}^{n+1} + [\mathrm{M}_\mathrm{D}]^{-1}\{\mathbf{D}\}^n \tag{32}$$

where the artificial dumping vector is given by

$$\{\mathbf{D}\}^n = \sum_E C_E \; C_{AD} \; S_E \; ([\mathrm{M}] - [\mathrm{M}_\mathrm{D}])_E \; \{\mathbf{U}\}^n \tag{33}$$

In Eq. (33) $C_E = \Delta t / \Delta t_E$ is the local Courant number, C_{AD} is an artificial dumping coefficient given by the user (in this work values between $0.4 \le C_{AD} \le 0.8$ were adopted for viscous fluids), S_E is a pressure sensor at element level obtained as an average of nodal values S_N. Values of S_N are components of the following assembled global vector

$$\{S\}^n = \frac{\sum_E \left| ([\mathrm{M}] - [\mathrm{M}_\mathrm{D}])_E \; \{p\}_E^n \right|}{\sum_E \left| ([\mathrm{M}] - [\mathrm{M}_\mathrm{D}])_E \right| \{p\}_E^n} \tag{34}$$

where the bars indicate the absolute value of the values inside matrices and, finally, [M] is the consistent mass matrix at element level, given by

$$[\mathrm{M}] = \int_{\Omega_E} [\Phi]^T [\Phi] \, d\Omega \tag{35}$$

In order to obtain all matrices and vectors indicated in Eqs. (20) to (30) and in Eq. (35) is necessary to calculate all the integer expressions involved. An analytical integration of those integer expressions was used in this work. To avoid the appearance of spurious modes the “h-stabilization method” was employed (Christon, 1997). Thus, an efficient FORTRAN code was developed and vectorized to run in a CRAY T94 of “Centro Nacional de Supercomputação na Região Sul” of “Universidade Federal do Rio Grande do Sul” in Brazil.

4. NUMERICAL EXAMPLE: "COLD" HYPERSONIC VISCOUS FLOW AROUND A DOUBLE ELLIPSOID

This example consists in a "cold hypersonic flow" of a viscous fluid over a double ellipsoid completed by a cylindrical extension as indicated in Fig. 1, where "cold hypersonic flow" means that the flow is hypersonic due its high velocity but no chemical reactions and molecular interactions are considered. This geometrical configuration is similar to a space shuttle and was also studied by Argyris et. al. (1989) within the Research and Developed Program for the Aerodynamics and Aerothermics of the European Space Project "Hermes". Due to flow symmetry with respect to the plane (x_1, x_3) only a half of complete domain has been considered.

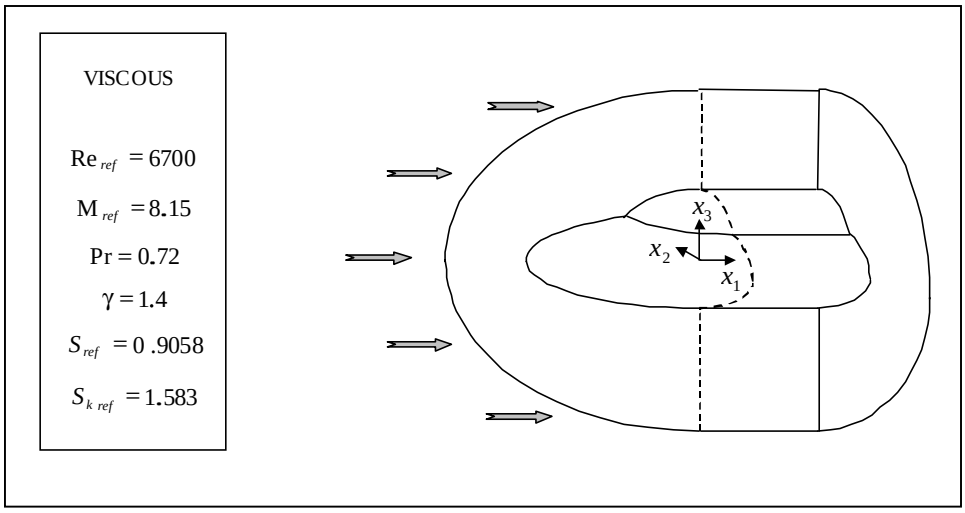

Figure 1 – "Cold" hypersonic flow around a double ellipsoid (α=0°)

The finite element mesh, containing 42746 elements and 46299 nodes, is shown in Figs. 2 and 3.

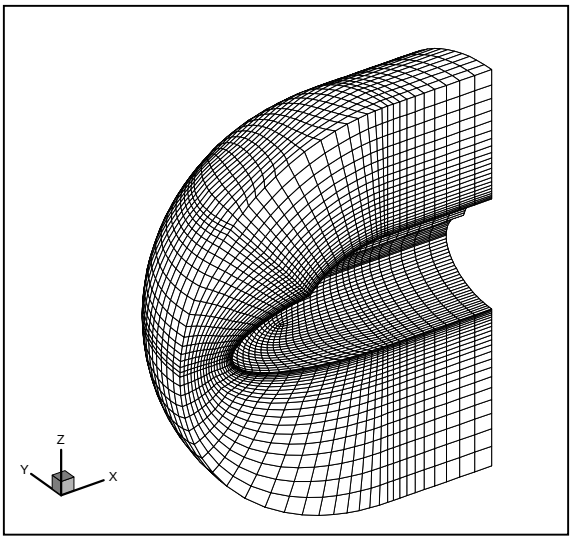

Figure 2 – Finite element mesh

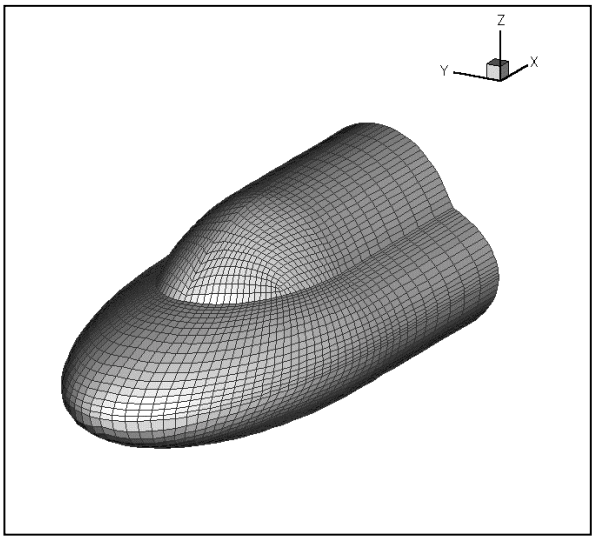

Figure 3 – Finite element mesh on the solid

The solid boundary is formed by two ellipsoids with two cylindrical extensions with

dimensionless length equal to 1.0. These ellipsoids are defined by the following equations

$$\left(\frac{x_1}{a}\right)^2+\left(\frac{x_2}{b}\right)^2+\left(\frac{x_3}{c}\right)^2=1 \quad \text{and} \quad \left(\frac{x_1}{l}\right)^2+\left(\frac{x_2}{m}\right)^2+\left(\frac{x_3}{n}\right)^2=1 \tag{36}$$

with $a=1.5$, $b=0.625$, $c=0.375$, $l=0.875$, $m=0.4375$, $n=0.625$. The external boundary, limiting the finite element domain, is characterized by an ellipsoid defined by the following equation

$$\left(\frac{x_1}{p}\right)^2+\left(\frac{x_2}{q}\right)^2+\left(\frac{x_3}{r}\right)^2=1 \tag{37}$$

with $p=2.0$, $q=1.0$, $r=1.8$.

The following prescribed inflow boundary conditions have been adopted

$$v_{1\infty}=8.15\ ;\ v_{2\infty}=v_{3\infty}=0.0\ ,\ u_{\infty}=1.7857\ ,\ \rho_{\infty}=1.0 \tag{38}$$

whereas on the solid boundaries the non-slip condition was applied, i.e. $v_1=v_2=v_3=0.0$. The following initial conditions were considered in the whole domain

$$v_1^{\,0}=8.15\ ;\ v_2^{\,0}=v_3^{\,0}=0.0\ ,\ u^0=1.7857\ ,\ e^0=35.0\ ,\ \rho^0=1.0 \text{ and } p^0=0.71428 \tag{39}$$

Using the safety factor $\beta=0.3$, the effective dimensionless time step employed in this example was $\Delta t=10^{-4}$. The tolerance adopted in the iterative process was $TOL=10^{-3}$ and the temporal tolerance was $TOL_t=10^{-5}$. The artificial dumping coefficient used here was $C_{AD}=0.8$.

Values of Mach number are presented in Fig. 4 whereas vectors representing the shear stress components on the solid boundary, used to compute the skin friction components, are shown in Fig. 5

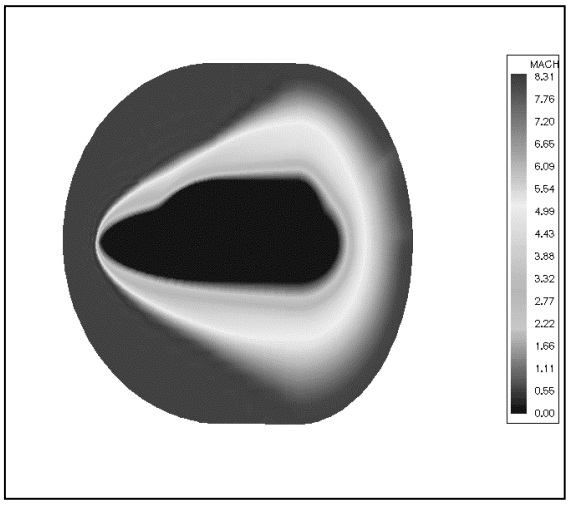

Figure 4 – Mach number distribution

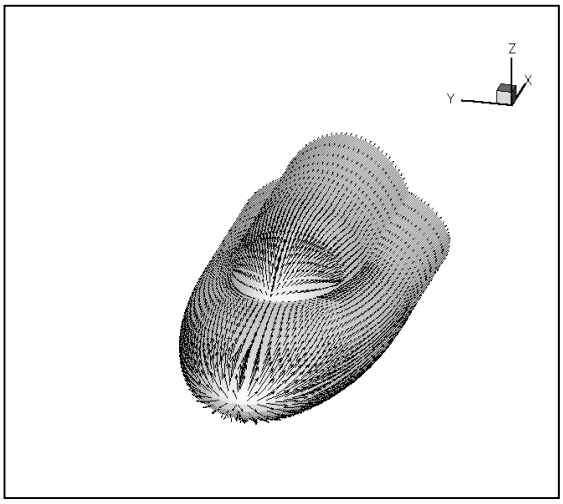

Figure 5 – Shear stresses (skin friction)

This example allows testing the program with a high compressible flow without considering the typical molecular interactions and chemical reactions that appear in hypersonic flows. Thus, it serves as a test example, selected in order to elucidate the

requirements posed on the finite element mesh, the performance of the present scheme and the efficiency of the codes and the entire model.

As a matter of fact it can be observed in Fig. 4 that the shock front is reproduced adequately by the present model. The viscous boundary layer in the vicinity of the body appears reasonably well defined as a result of the selected fine discretization in that region.

These results are very close to those obtained by Argyris et. al. (1989). A good performance was also obtained with regard to code vectorization (647 Mflops in a supercomputer CRAY T94).

Finally Fig. 6 shows the numerical behavior of the solution. Here may be observed that the density residuum decreases continuously as the number of time steps increases.

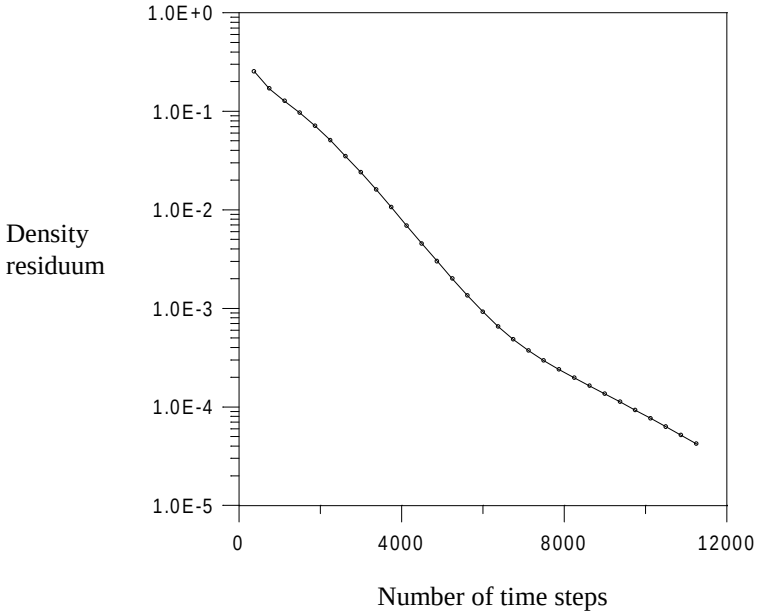

Figure 6 – Numerical behavior

5. CONCLUSIONS

A numerical algorithm to simulate high compressible flows was presented in this work using an iterative one-step Taylor-Galerkin scheme and the finite element method for space discretization. Evaluating the determinant and the inverse of the Jacobian matrix at the element centroid and solving the corresponding integrals, derived from the eight-node hexahedral isoparametric element, analytical expressions were obtained for the element matrices. Although this process requires to avoid strong mesh distortions and to use more elements that the classical procedure with full numerical integration, it becomes a very efficient technique for large-scale computations, especially when explicit algorithms are employed.

An example for “cold” hypersonic flow of a viscous fluid was presented and good agreements were obtained with regard to results presented in the correspondent reference. Excellent computational performance in terms of CPU time, memory savings and code vectorization were also obtained.

Acknowledgements

The authors wish to thank CNPq and CAPES for their financial support and to CESUP

(Centro Nacional de Supercomputação na Região Sul) for its technical support.

REFERENCES

Argyris, J., Doltsinis, I. S. & Friz, H., 1989, Hermes space shuttle: exploration of reentry aerodynamics, Computer Methods in Applied Mechanics and Engineering, vol. 73, pp. 1-51.

Christon, M. A., 1997, A domain-descomposition message-passing approach to transient viscous incompressible flow using explicit time integration, Computer Methods in Applied Mechanics and Engineering, vol. 148, pp. 329-352.

Donea, J., 1984, A Taylor-Galerkin method for convective transport problems, International Journal for Numerical Methods in Egineering, vol. 20, pp. 101-119.

Löhner, R., Morgan, R. & Zienkiewicz, O.C., 1985, An adaptive finite element procedure for compressible high speed flows, Computer Methods in Applied Mechanics and Engineering, vol. 51, pp. 441-465.

Löhner, R., 1988, Finite element flux corrected transport (FEM-FCT) for the Euler and Navier-Stokes Equations, Finite Elements in Fluids (Ed. by Gallagher et. al.), vol. 7, ch. 6, pp. 105-121.

Morgan, K., Peiraire, J. & Peiro, J., 1991, The computation of three-dimensional flows using ustructured grids, Computer Methods in Applied Mechanics and Engineering, vol. 87, pp. 335-352.

Richtmeyer, R. D. & Morton, K. W., 1967, Difference methods for initial value problems, Interscience, N.Y.

Texeira, P. R. F., Awruch, A. M. & Santos, M. A. V., 1998, Numerical simulation of three dimensional compressible flows using finite elements with mixed structured-unstructured grids, J. Brazilian Soc. Mech. Sciences, V xx, N° 1, pp. 62-78.

White, F., 1974, Viscous Fluid Flow, McGraw Hill Book Co. (Fist edition), N.Y.

Zienkiewicz, O. C. & Cheung, Y. K., 1965, Finite element method in the solution of field problems, The Engineer, vol. 24, pp 507-510.